Electron/Proton Coupling in Bacterial Nitric Oxide Reductase during Reduction of Oxygen†

Ulrika Flock,‡ Nicholas J. Watmough,§ and Pia Ädelroth*,‡

Department of Biochemistry and Biophysics, The Arrhenius Laboratories for Natural Sciences, Stockholm University, SE-10691 Stockholm, Sweden, and Centre for Metalloprotein Spectroscopy and Biology, School of Biological Sciences, University of East Anglia, Norwich, NR4 7TJ, U.K.

Received March 22, 2005; Revised Manuscript Received June 9, 2005

ABSTRACT: The respiratory nitric oxide reductase (NOR) from *Paracoccus denitrificans* catalyzes the two-electron reduction of NO to N_2O ($2NO + 2H^+ + 2e^- \rightarrow N_2O + H_2O$), which is an obligatory step in the sequential reduction of nitrate to dinitrogen known as denitrification. NOR has four redox-active cofactors, namely, two low-spin hemes *c* and *b*, one high-spin heme b_3, and a non-heme iron Fe_B, and belongs to same superfamily as the oxygen-reducing heme-copper oxidases. NOR can also use oxygen as an electron acceptor; this catalytic activity was investigated in this study. We show that the product in the steady-state reduction of oxygen is water. A single turnover of the fully reduced NOR with oxygen was initiated using the flow−flash technique, and the progress of the reaction monitored by time-resolved optical absorption spectroscopy. Two major phases with time constants of 40 μs and 25 ms (pH 7.5, 1 mM O_2) were observed. The rate constant for the faster process was dependent on the O_2 concentration and is assigned to O_2 binding to heme b_3 at a bimolecular rate constant of 2×10^7 M^{-1} s^{-1}. The second phase ($\tau = 25$ ms) involves oxidation of the low-spin hemes *b* and *c*, and is coupled to the uptake of protons from the bulk solution. The rate constant for this phase shows a pH dependence consistent with rate limitation by proton transfer from an internal group with a $pK_a = 6.6$. This group is presumably an amino acid residue that is crucial for proton transfer to the catalytic site also during NO reduction.

Bacterial NO-reductases (NOR[1]) are integral membrane proteins that reduce NO to N_2O (eq 1) as part of the denitrification process (for recent reviews, see refs *1*, *2*).

$$2NO + 2H^+ + 2e^- \rightarrow N_2O + H_2O \qquad (1)$$

The largest subunit in the NORs was shown by sequence alignments to be a divergent member of the superfamily of O_2-reducing heme-copper oxidases (HCuOs), which are characterized by having a catalytic subunit with six invariant histidines at the same predicted positions in 12 transmembrane helices (*3*, *4*). Two of these histidines coordinate a low-spin heme, one a high-spin heme and the remaining three histidines coordinate a copper ion in the heme-copper oxidases (hence the name). In NOR, this copper is presumed to be replaced by a non-heme iron (*5*, *6*).

In its purified form, the NOR from *Paracoccus* (*P.*) *denitrificans* contains two subunits: NorB and NorC. NorB is the catalytic subunit harboring a low-spin heme *b*, a high-spin heme b_3, and a non-heme iron, Fe_B. The heme b_3 and Fe_B form a magnetically coupled binuclear center, which is the site of NO reduction. NorC is a membrane-anchored protein harboring a low-spin heme *c*, which is believed to be the site of electron entry from the water-soluble electron source, in *P. denitrificans* either cytochrome (cyt) c_{551} or pseudoazurin (*1*).

The purified *P. denitrificans* NOR catalyses NO reduction with a maximum turnover number of ~40 $NO \cdot s^{-1}$ (*6*, *7*). The mitochondrial aa_3-type HCuOs, like bovine cytochrome *c* oxidase (C*c*O), are not capable of NO reduction at significant turnover rates, whereas the bacterial cbb_3-type HCuO's, which have the highest degree of sequence similarity with the NORs, also have the highest measured NO-reduction activity (~2 $NO \cdot s^{-1}$) among the HCuO's (*8*, *9*). The reason for the difference in NO-reduction capability among the HCuOs is not known, but has been suggested to be related to the affinity of Cu_B for CO, which is higher in at least some of the bacterial HCuOs capable of NO reduction than for the mitochondrial-like oxidases (*9*). The properties of NOR that differ from HCuOs, and thus might be involved in conferring the high NO-reducing capability, include (i) the iron instead of copper in the catalytic site (see below) and (ii) a very low midpoint potential of high-spin heme b_3 (*10*), possibly in order to avoid formation of a stable heme b_3^{2+}−NO "dead-end" complex during turnover (*10*). The detailed mechanism for NO reduction by NOR is not known, but models have been suggested that involve either a "trans" mechanism (*11*−*13*) where one NO binds

† This work was supported by grants from the Swedish Research council and the Magn. Bergwall foundation.

* Corresponding author. Tel: +46-8-164183. Fax: +46-8-153679. E-mail: piaa@dbb.su.se.

‡ Stockholm University.

§ University of East Anglia.

[1] Abbreviations: NOR, bacterial nitric oxide reductase; HCuO, heme-copper oxidase; C*c*O, cytochrome *c* oxidase; DDM, β-D-dodecyl maltoside; TMPD, *N*,*N*,*N*′,*N*′-tetramethyl-*p*-phenylenediamine; MES, 2-morpholinoethanesulfonic acid; HEPES, 4-(2-hydroxyethyl)-piperazine-1-ethanesulfonic acid; TRIS, tris(hydroxymethyl)aminomethane.

10.1021/bi050524h CCC: $30.25
Published on Web 07/12/2005

to each of the metals in the binuclear site, or a "cis" mechanism (*14*) where two NOs bind to the non-heme Fe_B. These models need to account for the observation that the maximum turnover activity is obtained at ~5 μM NO but at higher NO concentrations the activity decreases, possibly due to inhibition by NO binding also to oxidized heme b_3 (*6*, *15*).

The HCuOs (for reviews see e.g. refs *16*, *17*) catalyze the four-electron reduction of oxygen to water (eq 2), and use the free energy available from this reaction to generate an electrochemical proton gradient across the membrane.

$$O_2 + 8H^+_{in} + 4e^- \rightarrow 2H_2O + 4H^+_{out} \qquad (2)$$

The HCuOs generate this proton gradient by using protons derived exclusively from the "inside" (the mitochondrial matrix or bacterial cytoplasm) for water formation (substrate protons). In addition, the HCuOs couple the electron transfer from the electron donor (often a cyt *c*) to oxygen (E'_0 = +0.8 V) to the translocation of protons across the membrane. In contrast, available data indicate that the two-electron reduction of NO catalyzed by NOR is nonelectrogenic (*13*, *18*), i.e. not coupled to charge translocation across the membrane. This is surprising since the free energy available from the transfer of electrons from the electron donor to NO (E'_0 = +1.2 V) is even larger than for O_2 reduction. As electrons are supplied by soluble donors from the periplasmic side of the membrane, the lack of electrogenicity in NOR implies that the protons needed for NO reduction (see eq 1) are also taken from the periplasm. This means that NOR must contain a proton transfer pathway leading from the periplasmic side of the membrane into the catalytic site, which is buried in the lipid bilayer. The route of this pathway is not known, but mutagenesis studies have shown that Glu-125 and Glu-198 in NorB are required for normal steady-state NO-reduction activity (*7*). Modeling studies predict that these glutamates, which may be involved in proton transfer, are located close to the periplasmic surface (Glu-125), and in the middle of the membrane close to Fe_B (Glu-198) (*19*).

In addition to the physiological NO-reduction activity, the *P. denitrificans* NOR and the closely related enzymes from *Paracoccus pantotrophus* and *Paracoccus halodenitrificans* can catalyze the reduction of dioxygen with turnover numbers on the order of 2−10 electrons·s^{-1} (*7*, *20*, *21*), although it is not clear how widespread the ability to reduce dioxygen is among the bacterial NORs (see e.g. ref *22*). Studies of mutant forms of *P. denitrificans* NOR have shown that the O_2- and NO-reduction activities are well correlated (*7*). Thus, an amino acid substitution affecting the rate of NO reduction similarly influences the rate of O_2 reduction, showing that the same catalytic components are involved in both processes.

For the HCuOs, the detailed mechanisms of oxygen reduction, proton transfer to the catalytic site, and proton pumping have been extensively investigated using the so-called "flow−flash" technique (*23*). In this technique, fully reduced enzyme with carbon monoxide (CO) bound to the high-spin heme in the active site is mixed in a stopped-flow apparatus with an oxygenated solution. Since CO and O_2 bind at the same site, the reaction of the fully reduced enzyme with O_2 is limited by the dissociation rate of CO, which is slow. However, if a short laser flash (~10 ns) is applied ~100 ms after mixing, the photolabile Fe−CO bond is broken and the binding of dioxygen and its subsequent stepwise reduction can be followed using time-resolved (from nanoseconds) spectroscopy. The flow−flash technique has been used in combination with various detection techniques and has yielded a wealth of information about the catalytic cycle of the HCuOs, e.g. how fast different intermediates are formed, the chemical nature of these intermediates, the sequence of electron transfer reactions, and the mechanisms and pathways for proton transfer to the catalytic site and across the membrane (see e.g. refs *24*−*26*).

The flow−flash technique has also been used to study the reduction of NO by NOR (*13*). The reductive coupling of two NO molecules to form N_2O requires two electrons, whereas the fully reduced NOR has four redox-active groups. Hence two full turnovers are required to reoxidize the enzyme. Moreover, since after oxidation the oxidized heme b_3 can bind NO (see above and ref *15*), the multiple possible reaction paths in the reaction of fully reduced NOR with NO makes interpretation of results complicated.

In this work, we have studied the reaction of fully reduced NOR with O_2 using the flow−flash technique. The aim is twofold; first to use the O_2 reaction to study ligand binding, electron transfer, and proton transfer to the catalytic site of NOR. Since reduction of O_2 to H_2O consumes four electrons and four protons (eq 2), the fully reduced NOR should yield a single turnover with one O_2 molecule. Second, comparisons of the reactions of NOR and the HCuOs with the substrates NO and O_2 provide information about those structural elements that determine the substrate specificity. Moreover, because of the chemical reactivity of NO in aqueous solutions, direct measurement of proton consumption by NOR using pH-sensitive dyes in unbuffered solutions is not experimentally straightforward. In contrast, when O_2 serves as the oxidant, these reactions can be studied directly, providing a means to study the details of proton transfer into the catalytic site of NOR.

MATERIALS AND METHODS

Growth of Bacteria and Purification of NOR. The NOR used in this study was from *Paracoccus (P.) denitrificans*, expressed in *Escherichia (E.) coli* JM 109 using the expression system described in ref *7*. Growth of bacteria, preparation of membranes, and purification of NOR were essentially as described in ref *7*, with the following exceptions: The bacteria were grown in TB (terrific broth) (*27*), and Cu-IMAC chromatography (*5*) was not used since the extent of purification achieved using the Q-Sepharose (Pharmacia) anion exchanger is sufficient for these experiments. NOR purified in this fashion (A^{280}/A^{410} ratio 1.0−1.5) was concentrated on Amicon tubes (Millipore), and the buffer changed to 50 mM tris(hydroxymethyl)aminomethane (TRIS), pH 7.6, 0.05% (w/v) β-dodecyl-maltoside (DDM) by repeated dilution and reconcentration. NOR was then rapidly frozen in N_2(l) and stored at −80 °C until needed.

Steady-State O_2 Reduction. Oxygen consumption by NOR was measured using a Clark-type electrode (Hansatech) with horse-heart cyt *c* (Sigma) as the electron donor. The reaction medium contained either 20−60 μM reduced cyt *c* or a mixture of 20−60 μM cyt *c*, 5 mM ascorbate, and 1 mM *N*,*N*,*N*′,*N*′-tetramethyl-*p*-phenylenediamine (TMPD) in 50 mM KH_2PO_4, pH 6.5, 0.05% DDM. Cyt *c* oxidation was

measured optically at 550 nm using a Cary 400 spectrophotometer (Varian) with 20−60 μM reduced cyt *c*. Cyt *c* was reduced with hydrogen gas using platinum black as a catalyst (*28*).

Sample Preparation for Flash Photolysis and Flow−Flash Studies. NOR was diluted to 5−10 μM in a modified Thunberg cuvette, air was exchanged for nitrogen on a vacuum line, and the enzyme was reduced either by adding 1−2 mM ascorbate and 0.2 μM 5-methylphenazinium methosulfate (PMS) or by adding small amounts (10−80 μM) of sodium dithionite. The advantage of using dithionite as the sole reductant is that any excess dithionite is consumed by O_2 during the mixing time in the flow−flash experiment and no rereduction of NOR occurs on slower time scales. Nitrogen was then exchanged for either 100% or 5−10% CO. The lower CO concentration was used for the flow−flash studies to avoid CO recombination interfering with O_2 binding (see Results).

Flow−Flash Measurements. Flow−flash measurements were performed on a setup described in ref *29*. Briefly, fully reduced CO-bound NOR was mixed 1:5 with an oxygenated buffer in a modified stopped-flow apparatus (Applied Photophysics, U.K.). After a 300 ms delay, a 10 ns laser flash (Nd:YAG laser, Quantel) was applied, dissociating CO and allowing O_2 to bind and initiate the reaction. The time course of the reaction was studied from microseconds to seconds at different wavelengths in the Soret and α regions. Typically, at each wavelength, 3×10^4 data points were collected and the data set was then reduced to ∼1000 points by averaging over a progressively increasing number of points (logarithmic time scale).

For the pH-dependence measurements, the buffer concentration in the NOR solution before mixing, in the same 1:5 ratio, was decreased to 10 mM (HEPES at pH 7.5). The oxygenated solution contained 100 mM of either citrate (pH 5.0−6.0), 2-morpholinoethanesulfonic acid (MES) (pH 6.0−7.0), 4-(2-hydroxyethyl)-piperazine-1-ethanesulfonic acid (HEPES) (pH 7.0−8.0), or TRIS (pH 8.0−9.0) depending on the final pH required. Since this procedure leaves only 300 ms for NOR to equilibrate with the new pH (the time between the mixing and the flash), we also incubated a NOR sample in 100 mM MES at pH 6.0 before mixing (with the same buffer), and no significant differences in the obtained results were observed compared to the described procedure.

Proton Uptake Measurements. To be able to measure pH changes during the flow−flash reaction with O_2, the buffering capacity of the sample was lowered by passing it through a PD-10 column (Pharmacia) equilibrated in 50 mM KCl, 0.05% DDM, 50 μM EDTA, pH ∼7.5. Phenol red at 40 μM was then added to the sample, which was reduced (with ascorbate/PMS) and CO-equilibrated as above. If necessary, the pH was readjusted to ∼7.5 as judged by the optical absorbance of the dye. In the flow−flash experiment, the O_2-saturated solution contained 50 mM KCl, 0.05% DDM, 50 μM EDTA, and 40 μM phenol red at pH ∼7.5. Phenol red has a broad pH-sensitive absorbance peak at 560 nm, but absorbance changes were monitored at 570 nm (see Results) to avoid interference from absorbance changes due to oxidation of the low-spin heme *b*, which has a maximum at 560 nm. To correct for the residual contribution from the redox reactions to the observed signal at 570 nm, traces were also collected in the presence of buffer (where there is no response from the pH-sensitive dye). The trace obtained in the presence of buffer was then subtracted from that obtained in the absence of buffer. In order to calibrate the observed dye signals in terms of $\Delta[H^+]$ consumed, the exhaust from the flow−flash apparatus was collected, placed in a cuvette under N_2, and adjusted (if necessary) to pH ∼7.5. Subsequently the buffering capacity of the solution ($\Delta A^{570}/\Delta[H^+]$) was measured by adding known amounts of HCl and recording the changes in absorbance at 570 nm.

Data Handling and Analysis. To extract the rate constants and kinetic difference spectra of the observed phases in the flow−flash reaction, the time-resolved changes in absorbance, measured at different wavelengths, were fitted either separately or globally to a model of consecutive irreversible reactions (e.g. A → B → C) using the software package Pro-K (Applied Photophysics, U.K.).

Table 1: Steady-State Oxygen Reduction by NOR with Cyt *c* as the Electron Donor[a]

pmol of O_2/ (s·pmol of NOR)	pmol of cyt *c*/ (s·pmol of NOR)	e^-/O_2
0.64 ± 0.05	2.7 ± 0.1	4.2 ± 0.4

[a] The activity was measured using both an oxygen electrode (O_2 consumption) and optical spectroscopy (cyt *c* oxidation). Note that four electrons are consumed per O_2 reduced, indicating that water is the product. Experimental conditions: 50 mM KH_2PO_4, pH 6.5, 0.05% DDM, 10−50 nM NOR, 20−60 μM reduced cyt *c* (with ascorbate and TMPD for some O_2 measurements, see Materials and Methods).

RESULTS

Steady-State O_2 Reduction by NOR. It is known that the *P. denitrificans* NOR is capable of O_2 reduction (*7*, *20*), but the product of the reaction has not been unambiguously determined. To determine whether O_2 is reduced to H_2O ($O_2 + 4H^+ + 4e^- \rightarrow 2H_2O$) or H_2O_2 ($O_2 + 2H^+ + 2e^- \rightarrow H_2O_2$), we measured O_2 reduction and cytochrome *c* oxidation under the same conditions. This allowed us to determine how many electrons are taken from cyt *c* per O_2 reduced, and the results are presented in Table 1. Four electrons are used per O_2 reduced, and hence H_2O is the product of the reaction. Moreover, including catalase in the O_2-reduction assays had no effect on the O_2 levels or rate of consumption (data not shown), supporting the conclusion that H_2O_2 is not formed.

CO Recombination to the Fully Reduced NOR. CO recombination to the reduced high-spin heme b_3 after flash photolysis of the CO-bound fully reduced NOR in an anaerobic CO atmosphere was studied as a probe of the integrity of the catalytic site. The CO recombination was biphasic with second-order rate constants of $\sim 2 \times 10^8$ M^{-1} s^{-1} and $\sim 2 \times 10^7$ M^{-1} s^{-1}. These values are very similar to those observed for the native *P. denitrificans* NOR (*30*). The contribution from the slower phase was ∼40% (slightly dependent on preparation) compared to ∼25% reported by Hendriks et al. for the native enzyme (*30*).

Single Turnover O_2 Reduction by the Fully Reduced NOR. Since NOR harbors four redox-active cofactors and oxygen is reduced to H_2O (see above), the fully reduced NOR should be capable of one complete turnover with O_2, making the system suitable for application of the "flow−flash" technique (see introduction). For the flow−flash technique to work, a number of conditions have to be fulfilled: First, the

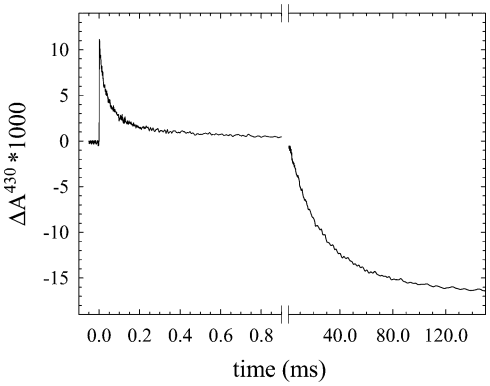

FIGURE 1: Absorbance changes at 430 nm upon flash photolysis of fully reduced CO-bound NOR in the presence of 1 mM O_2. The trace shows the two observed phases with time constants of ~40 μs and 25 ms. Experimental conditions: ~1 μM reacting NOR in 100 mM HEPES−KOH, pH 7.5, 50 mM KCl, 0.05% DDM, $[O_2] = 1$ mM, $T = 295$ K. The laser flash at $t = 0$ gives an artifact that has been truncated for clarity.

spontaneous dissociation of CO (the CO off rate) from the reduced high-spin heme must be slow enough to allow for mixing in the stopped-flow apparatus before the laser flash is applied. Second, after dissociation of CO by the flash, the rate of oxygen binding to the heme has to be faster than that of CO recombination. In the case of bovine C*c*O, the CO off reaction has a rate constant of ~0.023 s^{-1} in the dark (*23*), O_2 binding a second order rate constant of 1.2×10^8 M^{-1} s^{-1} (*31*, *32*), and CO rebinding an apparent second order rate constant of $\sim 7 \times 10^4$ M^{-1} s^{-1}. Consequently, upon mixing a CO-saturated (1 mM CO) C*c*O solution at a ratio of 1:5 with an O_2-saturated (1.2 mM O_2) solution, O_2 binding is 10^4 times faster than CO rebinding, and 300 ms after mixing (at the time of the flash), only ~1% of the C*c*O population is oxidized.

In order to determine the apparent CO off rate constant for NOR, we mixed the fully reduced CO-bound NOR with an O_2-saturated solution and measured the oxidation rate in the absence of any applied laser flash. Assuming that the oxidation phases are faster than CO dissociation, the reaction between NOR−CO and O_2 will be limited by the dissociation of CO. The observed kinetics was biphasic, with the faster process exhibiting a rate constant of ~0.5 s^{-1} under our measuring light conditions (data not shown). Consequently, at the time of the laser flash (at the latest ~300 ms after mixing), at most ~14% of the NOR population is already oxidized. The rapid CO-rebinding to the b_3 heme in NOR of 2×10^8 M^{-1} s^{-1} (see above and ref *30*) poses experimental problems since at a starting concentration of 1 mM CO, after mixing 1:5 in the flow−flash apparatus, the observed CO-rebinding time constant would be ~30 μs. Since O_2 binds to heme b_3 with a $\tau = 40$ μs at 1 mM O_2 (see next section), in order to have O_2 binding at least an order of magnitude faster than CO recombination, the CO concentration was lowered to ~50 μM before mixing.

In the flow−flash experiment with fully reduced NOR and O_2, after CO dissociation we observed two major kinetic phases in the time range 1 μs to 0.3 s in the visible region of the spectrum. Figure 1 shows the trace obtained at 430 nm, where both phases are clearly seen. The rapid (τ = 40 μs) phase we assign to oxygen binding to heme b_3, and the slower ($\tau = 25$ ms) to proton-coupled electron transfer

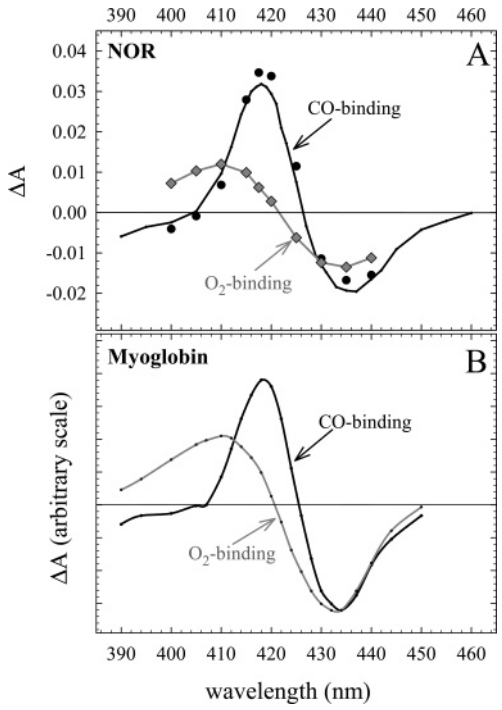

FIGURE 2: (A) The amplitudes at different wavelengths (kinetic difference spectrum) for the $\tau = 40$ μs (O_2-binding) phase (gray diamonds) and the kinetic difference spectrum for CO binding obtained by recording the amplitude for CO rebinding to reduced heme b_3 after flash-induced dissociation of CO in a CO atmosphere (−). Shown for comparison are also the amplitudes for CO dissociation (the "CO step") in the flow−flash experiment (●), multiplied by −1 to correspond to CO binding. Experimental conditions as in Figure 1. (B) The corresponding spectra for myoglobin reported by Verkhovsky et al. (*32*), showing the similarity to those obtained for NOR.

from the low-spin hemes *b* and *c* to the binuclear site. Both phases are discussed in more detail below. The progress of the reaction in our flow−flash experiments (see below) with the *P. denitrificans* NOR expressed in *E. coli* showed no major differences to that observed with the native *P. denitrificans* NOR (Flock, Thorndycroft, Watmough, and Ädelroth, unpublished).

O_2 Binding to Heme b_3. When mixing the fully reduced CO-bound ([CO] ≈ 50 μM) NOR (5−10 μM) at a ratio of 1:5 with an oxygen-saturated ($[O_2] = 1.2$ mM) buffer, the first phase observed after CO dissociation has a time constant of ~40 μs (see Figure 1). No electron transfer from the low-spin hemes occurs in this reaction. We assign this phase to oxygen binding to heme b_3 because (i) its optical kinetic difference spectrum (Figure 2A) is very similar to the corresponding ($Fe^{2+}-O_2$ minus Fe^{2+}) difference spectrum for myoglobin (Figure 2B) (*32*) and (ii) the observed rate constant for this phase depends on the O_2 concentration (Figure 3). From Figure 2A it is also seen that the initial spectral changes upon dissociating CO in the presence of O_2 (the "CO step") are very similar to the corresponding changes upon dissociating CO in the absence of O_2 (data from the CO-recombination experiment, see above), indicating that there are no significant unresolved phases preceding the $\tau = 40$ μs phase. Neither the rate constant nor amplitude of the O_2-binding phase was dependent on pH (data not shown).

In order to determine the second-order rate constant for O_2 binding to reduced heme b_3 we studied the kinetics of

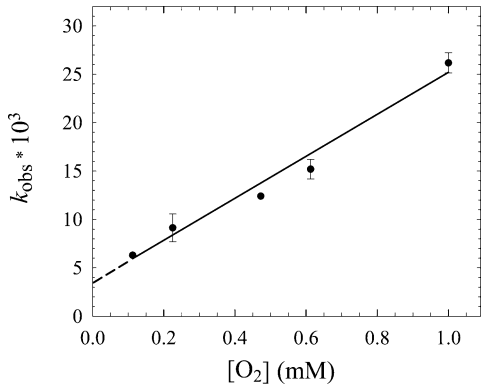

FIGURE 3: The rate constant for O_2 binding to NOR as a function of the O_2 concentration. When more than one measurement was made for the same [O_2], the data point shown is the mean value and the error bars correspond to the standard deviation. The solid line is a least-squares fit to the data, where the slope is the bimolecular rate constant k_{on} for O_2 binding at 2×10^7 M^{-1} s^{-1}. The dashed line is an extrapolation to [O_2] = 0, corresponding to an off rate constant for O_2, k_{off} (O_2) = ~3500 s^{-1}. Experimental conditions as in Figure 1.

O_2 binding at O_2 concentrations ranging from ~100 μM to 1.0 mM (Figure 3). Since the experiments were done under pseudo-first-order conditions, i.e. [O_2] ≫ [NOR], we fitted the experimental data to eq 3. The fit is shown in Figure 3

$$k_{obs} = k_{on}[O_2] + k_{off} \quad (3)$$

and gave a second-order rate constant for O_2 binding, k_{on}, of ~2×10^7 M^{-1} s^{-1}. Extrapolating the fitted line to [O_2] = 0 gave a k_{off} for O_2 of ~3500 s^{-1}, yielding a dissociation constant, $K_D = k_{off}/k_{on}$, for the b_3−O_2 complex of ~150 μM. We could not use O_2 concentrations much below ~100 μM because, at lower O_2 concentrations, interference from rebinding of CO becomes a problem.

Proton-Coupled Electron Transfer (the τ = 25 ms Phase). The second major phase in the reaction between fully reduced NOR and oxygen has a time constant of ~25 ms (k = 40 s^{-1}) at pH 7.5 (see Figure 1). The kinetic difference spectrum of this phase (Figure 4) shows substantial oxidation of both low-spin hemes, seen most clearly in the α region where the reduced minus oxidized spectrum of heme *b* has its peak at 560 nm, and that of heme *c* has a narrow peak at 552 nm. We therefore assign this phase to decay of the b_3^{2+}−O_2 species by electron transfer from the low-spin hemes *b* and *c* to the catalytic site. The amplitude of the 25 ms phase corresponds to 40 ± 10% oxidation of both low-spin hemes (see Discussion). In the Soret region, the sum of the kinetic difference spectra for the 40 μs phase (O_2 binding) and the 25 ms phase corresponds quite well with a static overall oxidized minus reduced spectrum (Figure 4), but see Discussion. The rapid phases of CO dissociation and O_2 binding were not resolved in the α region, but the sum of the absorbance changes for these processes were small compared to the amplitude of the 25 ms phase.

The rate constant for this phase (τ = 25 ms at pH 7.5) was found to decrease at higher pH (see Figure 5), in a way that could be well fitted by a simple Henderson−Hasselbalch equation (solid line in Figure 5), yielding a pK_a of ~6.6 and maximum rate constant at low pH of ~250 s^{-1}.

Proton Uptake. Proton uptake from solution was observed with the same rate constant as the 25 ms phase (pH 7.5),

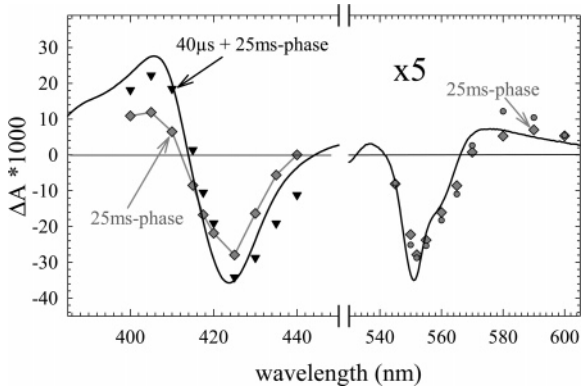

FIGURE 4: Kinetic difference spectrum for the τ = 25 ms (at pH 7.5) phase (gray diamonds) in the reaction between fully reduced NOR and O_2, shown both in the Soret and α (multiplied by a factor of 5) regions of the spectrum. In the Soret region, where O_2 binding contributes significantly to the total absorbance changes, the sum of the 40 μs and the 25 ms phases is also shown (▼). In the α region, where the τ = 40 μs phase was not resolved, the total absorbance changes (after 25 ms phase minus before flash) are shown (gray circles). For comparison, the static oxidized−reduced spectrum (−) is also shown. Experimental conditions as in Figure 1.

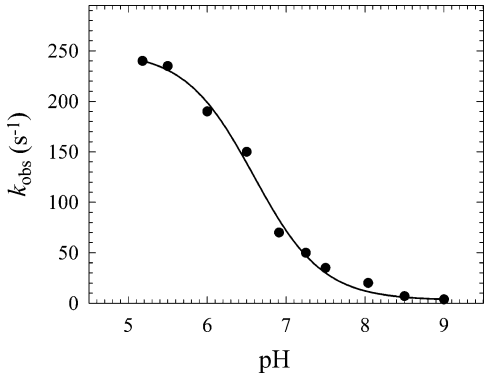

FIGURE 5: The pH dependence of the τ = 25 ms (k = 40 s^{-1}) phase. Shown are the rate constants obtained from a single-exponential fit to the data at each pH (●), and the line is a fit to eq 4, giving a k_{max} = 250 s^{-1} and a pK_{AH} = 6.6. Experimental conditions as in Figure 1, except for the buffers used in the pH titration: citrate (pH 5.0−6.0), MES (pH 6.0−7.0), HEPES (pH 7.0−8.0), TRIS (pH 8.0−9.0).

measured using the pH-sensitive dye phenol red at 570 nm (see Figure 6). This wavelength was chosen because it is close to the isobestic point in the oxidized−reduced spectrum of NOR (see Figure 4 and Figure 6). It is also clear from Figure 6 that the CO dissociation and O_2-binding reactions are not coupled to proton uptake/release from/to solution, since no changes in dye absorbance are seen faster than the 25 ms phase.

Using the determined buffering capacity ($\Delta A^{570}/\Delta[H^+]$) of the sample and the extinction coefficient of ~48 mM^{-1} at 418 nm obtained for the CO photolysis reaction (*30*) to calculate the concentration of reacting NOR in the flow−flash proton uptake experiment (see Discussion), ~1 H^+/reacting NOR is taken up in the 25 ms phase.

Slower Reactions. In addition to the τ = 40 μs and τ = 25 ms phases described above, there is a slower phase in the flow−flash reaction with a time constant of 1−2 s and a kinetic difference spectrum corresponding to further oxidation of the low-spin hemes. This phase overlaps in time (see above) with oxidation of the NOR molecules that are still CO-bound (due to our setup yielding less than

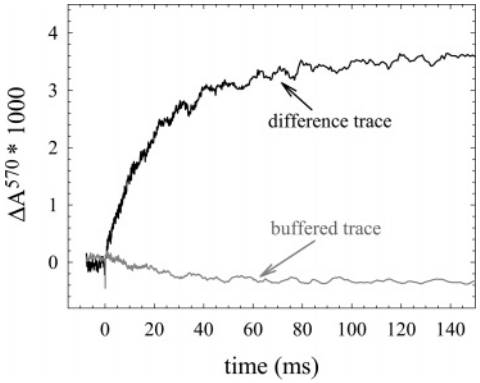

FIGURE 6: Proton uptake by NOR from the bulk solution during the $\tau = 25$ ms phase, measured at 570 nm and pH ~7.5 using the pH-sensitive dye phenol red. The graph shows the small absorbance changes observed in the presence of 20 mM HEPES (in gray) and the difference trace (in black) obtained after subtracting the buffered trace from the one obtained in the absence of buffer (see Materials and Methods for details). Experimental conditions: 50 mM KCl, 0.05% DDM, 50 μM EDTA, 40 μM phenol red, $[O_2] = 1$ mM, $T = 295$ K. A laser flash artifact around $t = 0$ has been truncated for clarity.

100% photolysis efficiency). We can thus not assign the slow ($\tau = 1-2$ s) phase unambiguously, but it could be the final step in the reaction, producing fully oxidized NOR and H_2O.

DISCUSSION

In this study we have investigated the reaction of bacterial NOR with oxygen. The product in the steady-state reduction of O_2 by NOR with cyt *c* as the electron donor was found to be H_2O. This implies that fully reduced NOR, which has four redox-active cofactors, most likely will bind one molecule of O_2 and completely reduce it to H_2O, leaving the NOR fully oxidized. These properties allowed us to use the "flow−flash" technique to investigate the mechanism of dioxygen reduction by fully reduced NOR. The experiments not only contribute to our understanding of the mechanism of NO reduction, but in addition form the basis for future studies using site-directed mutant forms of NOR to investigate the detailed mechanism of proton transfer in NOR, as O_2 is a more suitable oxidant than NO to use in combination with pH-sensitive dyes.

It has been observed that the static CO difference spectrum for NOR is different from the kinetic spectrum obtained upon photolysis of CO, and that initial CO binding to heme b_3 is much slower than rebinding after flash photolysis (*30*). These observations imply that the reduced heme b_3 is in a state after flash photolysis of CO that is different from the initially reduced state. It was suggested that this difference is due to a sixth ligand bound to heme b_3 in the initially reduced enzyme, the dissociation of which has to precede CO binding ((*30*), but see ref *33*). After CO photolysis, however, this sixth ligand cannot rebind because CO recombination with reduced heme b_3 is too fast. Consequently, the reduced NOR after flash-induced dissociation of CO in our flow−flash experiments is probably in a different state than the initially reduced enzyme, so that since O_2 binding is fast, the reaction presumably never proceeds through the initially reduced state. During physiological turnover with NO, the steady-state concentration of reduced b_3 is presumably quite low because

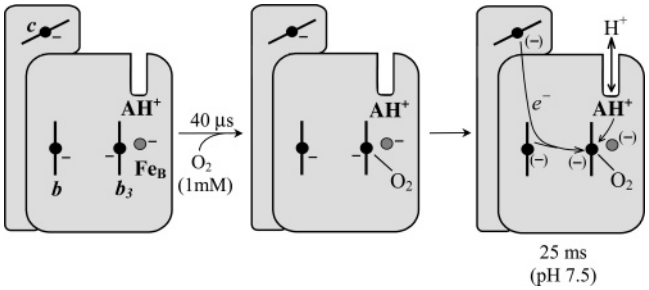

FIGURE 7: Summary of the reactions occurring during the $\tau = 40$ μs and $\tau = 25$ ms phases observed in the reaction between fully reduced NOR and O_2. The minus sign denotes a reduced site. After dissociation of CO, O_2 binds to the "open" position of heme b_3 with $\tau = 40$ μs. During the $\tau = 25$ ms phase, we observe (partial) oxidation of all hemes. Presumably also the Fe_B is oxidized although this site is not visible in our experiments. The group AH ($pK_{AH} = 6.6$) is presumed to be in equilibrium with the bulk solution throughout the reactions, but this equilibrium is shown only during the $\tau = 25$ ms phase when there is a change in bulk proton concentration as the proton on AH is transferred on to the binuclear site. See text for details.

of its low midpoint potential of ~60 mV (*10*). Consequently, since NO binding to reduced b_3 is very rapid (10^9 M^{-1} s^{-1} (*13*)), it is probable that the "resting" form of initially reduced heme b_3 is not populated significantly during turnover and that the reduced species after flash photolysis of CO in our experiments is more physiologically relevant. The reactions occurring in the two major phases observed in our flow−flash experiments are summarized in Figure 7 and discussed below.

Reaction of Fully Reduced NOR with Oxygen. The first phase observed in the reaction of fully reduced NOR with O_2, $\tau = 40$ μs at 1 mM O_2, occurs without electron transfer from the low-spin hemes. Although we at this point cannot exclude that fractional electron transfer from the binuclear site occurs in this phase, we assign it to formation of a ferrous−oxy complex at heme b_3 (see Figure 7). This assignment is based on the kinetic difference spectrum (see Figure 2A) which is similar in form, but shifted in wavelength compared to the CO difference spectrum. These CO-binding and O_2-binding spectra for NOR are very similar to the corresponding spectra for myoglobin (Figure 2B) (*32*), indicating that Fe_B is not involved in the observed NOR−O_2 complex. The spectrum for O_2 binding to NOR is also very similar to the spectrum obtained for NO binding to NOR (*13*). The amplitude of the absorbance changes attributed to O_2 binding to NOR, compared to the CO off absorbance changes, indicates that a significant fraction of heme b_3 binds O_2 (at 1 mM O_2), consistent with the obtained K_D of ~150 μM. In C*c*O, the relative amplitude for the absorbance changes associated with O_2 binding (compared to CO off absorbance changes) is considerably smaller than that for myoglobin (*32*), indicating a higher K_D for O_2 in C*c*O than in NOR. The K_D of O_2 binding to heme a_3 in C*c*O has been estimated at several mM (*32*), but direct measurements such as those presented here are hampered by the rapid electron transfer (in bovine C*c*O, τ(ET) ≈ 35 μs, only ~4 times slower than O_2 binding ($\tau = 8$ μs at 1 mM O_2)) from the low-spin heme, trapping the bound oxygen (*34*) and leading to low apparent K_D values. In the reaction of NOR with O_2, these direct measurements are possible since the heme oxidation takes place with a $\tau = 25$ ms (pH 7.5),

separating it from oxygen binding ($\tau = 40$ μs at 1 mM O_2) by almost 3 orders of magnitude. It should also be noted that O_2 binding to NOR is monophasic (at our signal-to-noise ratio) and neither the rate constant nor the amplitude is dependent on the pH (data not shown). This is in contrast to CO recombination with the fully reduced NOR, which is biphasic, with the relative ratios for the faster and slower phases changing with pH (Ädelroth, unpublished). Taken together, these results indicate that the biphasic reaction with CO is not due to a general heterogeneity, but that there are two conformations for CO binding that involve protonatable groups, whereas there is less flexibility in the heme b_3 pocket for oxygen binding than for carbon monoxide. Neither CO dissociation nor O_2 binding was coupled to any significant proton uptake/release (see Figure 6), so the small electrogenic response observed previously upon CO photolysis (*13*) must be due to a charge movement that is not propagated to the bulk solution.

The second phase observed in the flow−flash reaction ($\tau = 25$ ms), involving oxidation of the low-spin hemes *b* and *c*, is coupled to proton uptake from the bulk solution, and discussed in detail below.

The $\tau \approx 1-2$ s ($k = 0.5-1$ s^{-1}) phase, also involving oxidation of the low-spin hemes, is possibly the final phase in the reaction, forming H_2O at the catalytic site. This slow phase could be limited by returning of the μ-oxo bridge between the oxidized heme b_3 and Fe_B that has been observed in the "resting" oxidized state (*35*, *36*). In the flow−flash reaction the bound O_2 requires four electrons for full reduction, which means that a slowest rate constant of 0.5−1 s^{-1} corresponds to 2−4 e^- s^{-1}, which is similar to the turnover rate (see Table 1) and could be the overall rate-limiting step. It should be noted that if the slow phase is the final step in the reaction, reducing the oxygen intermediate formed at the binuclear site by oxidizing the remaining reduced low-spin hemes (the $\tau = 25$ ms phase corresponds to ~40% oxidation of low-spin hemes, see Results), then the kinetic difference spectra for the $\tau = 25$ ms phase and the $\tau = 1-2$ s phase should differ. This is because the $\tau = 25$ ms phase should then presumably include oxidation of heme b_3 (and Fe_B, not visible in our experiments) in addition to the low-spin hemes, whereas the slow $\tau = 1-2$ s phase should only involve oxidation of the remaining fraction low-spin hemes. In the kinetic difference spectrum of the sum of the $\tau = 40$ μs and the $\tau = 25$ ms phase shown in Figure 4, there is a shift toward longer wavelengths compared to the static reduced−oxidized spectrum, which would indicate oxidation of a larger fraction heme b_3 than hemes *b* and *c* in this phase. This shift is not seen in the kinetic difference spectrum for the $\tau = 1-2$ s phase (data not shown), supporting the possible interpretation that it is the final phase in the reaction. Hence, our tentative assignment of the two oxidation phases is that in the $\tau = 25$ ms phase the electrons on b_3 and presumably Fe_B together with one electron from the heme *c*/*b* equilibrium are used (see Figure 7) to form a formally three-electron-reduced intermediate at the binuclear site. This intermediate then decays with $\tau = 1-2$ s upon transfer of the last electron from hemes *c*/*b* to the binuclear site.

Proton Transfer into the Heme b_3−Fe_B Site. The time constant for proton uptake by NOR ($\tau = 25$ ms at pH 7.5) observed in the flow−flash reaction with O_2 is in the same time range as the kinetic phases assigned to proton uptake (with time constants of ~2 and 10 ms) in the reaction of fully reduced NOR with NO (*13*). The chemical proton-coupled side reactions of NO in water (*13*) hamper the use of NO in combination with the unbuffered solutions needed for the direct measurements of proton uptake using pH-sensitive dyes. There is thus an experimental advantage to studying the reaction of NOR with O_2, and this reaction can be used to gain insight into the mechanism of proton transfer into the catalytic site in NOR.

Since the full reduction of O_2 to H_2O requires four protons, determining the amount of protons/NOR (β) taken up in the oxidative phase studied here also gives the number of protons/NOR taken up in the reductive phase ($4 - \beta$). The determination of β requires relating the change in proton concentration during oxidation (see Materials and Methods) to the concentration of NOR participating in the reaction. For the HCuO flow−flash studies, this is done by using the initial absorbance change due to CO photolysis (the "CO step") as the "ruler", with the static CO difference spectrum extinction coefficients giving the concentration of reacting enzyme (see e.g. ref *37*). This is not straightforward for NOR since, as discussed above, the static CO difference spectrum and the kinetic spectrum obtained upon flash-induced CO dissociation are not identical ((*30*); Ädelroth, unpublished). On the basis of the extinction coefficient at 418 nm obtained for the CO photolysis reaction (*30*) of ~48 mM^{-1} cm^{-1}, ~1 H^+/reacting NOR is taken up in the 25 ms phase. As discussed above, the 25 ms phase does not correspond to full oxidation of the low-spin hemes *b* and *c*, so that relating instead the amount of protons consumed to the concentration of low-spin hemes oxidized gives $\beta = 2.5 \pm 0.5$ H^+/fully oxidized NOR. If we assume the same stoichiometry of electron/proton coupling in the slower ($\tau = 1-2$ s) phase, then 1.5 ± 0.5 H^+ ($4 - \beta$) are taken up during reduction of oxidized NOR, one of them presumably needed to release the μ-oxo bridge between b_3 and Fe_B.

The pH dependence of the 25 ms phase (Figure 5) shows a saturating rate constant at low pH, and the rate constant then decreases with increasing pH. This behavior excludes a mechanism involving direct proton transfer from the bulk solution to the binuclear site since in this case the rate constant would not saturate at lower pH. The pH dependence is instead consistent with a model for a two-step process (eq 4, see also Figure 7), where a rate-limiting internal proton transfer from a group AH is followed by rapid reprotonation of A^- from the bulk solution.

$$k_{obs}(\mathrm{pH}) = \alpha_{AH}(\mathrm{pH})\, k_H \tag{4a}$$

$$\alpha_{AH}(\mathrm{pH}) = \frac{1}{1 + 10^{\mathrm{pH}-\mathrm{p}K_{AH}}} \tag{4b}$$

In this model, the observed rate constant, k_{obs}, is determined by the fraction of the internal group that is in the protonated form, α_{AH}, determined by the pK_{AH} and the pH (eq 4b), multiplied by the rate constant of internal proton transfer (k_H) from AH to the binuclear site (eq 4a). Fitting the experimental data to this model (shown in Figure 5) gives a value for $k_H = 250$ s^{-1} and a pK_{AH} of 6.6. This model (eq 4a) predicts that the rate constant falls toward zero at high

pH, which is consistent with our data. We can, however, not exclude that there is a small contribution from a pH-independent rate ($<3\ s^{-1}$) since at slow rates there is overlap with the $\tau = 1-2$ s phase. The $\tau = 25$ ms phase also involves electron transfer from the low-spin hemes to the binuclear site. Equilibration of electrons between hemes *b* and *c* occurs with an observed rate constant $k = 3 \times 10^4\ s^{-1}$, and equilibration between hemes *b* and b_3 is even faster (*13*). Consequently, electron transfer is assumed not to be rate limiting for the $\tau = 25$ ms phase. However, it should be noted that it is possible that the rate of the proton-coupled electron transfer is also dependent on the fraction reduced binuclear site, which is determined by the relative midpoint potentials of the redox sites (cf. the model for the last phase in the corresponding reaction for C*c*O (*38*)). This could provide an explanation as to why the rate constants for the processes assigned to proton-coupled electron transfer in the reaction of fully reduced NOR with NO are faster than with O_2 as the oxidant. In this case, presumably the midpoint potential of the binuclear site with NO bound is higher than with O_2, leading to a larger fraction reduced binuclear site and hence a faster rate.

It is possible that proton transfer from the $pK_a = 6.6$ group observed in our experiments is involved in limiting the turnover rate in steady-state NO reduction by NOR, since the turnover activity is strongly pH dependent in a range where this residue titrates (pH = 6−8) (*35*). Interestingly, the proton transfer rate constant ($\tau = 25$ ms, $k = 40\ s^{-1}$) we observe at pH 7.5 corresponds well with the turnover activity with NO measured around the same pH ($30-80\ s^{-1}$, see e.g. refs *13*, *35*). There are presumably also other important titratable groups since the optimum pH for turnover with NO has been measured to be pH ≈ 5 (*22*, *39*). The identity of the $pK_a = 6.6$ group is unknown, but there are several protonatable amino acid residues that are predicted to be close to the binuclear site or in the region above the hemes (*19*) which should provide a proton transfer pathway into the binuclear site. The effect on the catalytic activity of changing some of these residues was studied by using site-directed mutagenesis (*7*), and Glu-125 and Glu-198 in NorB were found to be essential for normal steady-state NO-reduction activity. These glutamates are predicted to be located close to the periplasmic surface (Glu-125) and in the middle of the membrane close to Fe_B (Glu-198). Consequently, it is possible that these residues are involved in proton transfer into the catalytic site, and that one of them is the group with $pK_a = 6.6$ that we observe in this work. The work presented here thus forms a platform for investigations of variant forms of NOR, in which protonatable residues potentially involved in proton delivery to the catalytic site have been modified, in order to elucidate the mechanism and pathway for proton transfer in NOR.

ACKNOWLEDGMENT

We are grateful to Professors Peter Brzezinski (Stockholm University) and David J. Richardson (University of East Anglia) for valuable discussions and to Dr. Sarah Field (University of East Anglia) for advice on purification of the NOR.

REFERENCES

1. Zumft, W. G. (2005) Nitric oxide reductases of prokaryotes with emphasis on the respiratory, heme-copper oxidase type, *J. Inorg. Biochem. 99*, 194−215.
2. Watmough, N. J., Butland, G., Cheesman, M. R., Moir, J. W., Richardson, D. J., and Spiro, S. (1999) Nitric oxide in bacteria: synthesis and consumption, *Biochim. Biophys. Acta 1411*, 456−474.
3. Saraste, M., and Castresana, J. (1994) Cytochrome oxidase evolved by tinkering with denitrification enzymes, *FEBS Lett. 341*, 1−4.
4. van der Oost, J., de Boer, A. P., de Gier, J. W., Zumft, W. G., Stouthamer, A. H., and van Spanning, R. J. (1994) The heme-copper oxidase family consists of three distinct types of terminal oxidases and is related to nitric oxide reductase, *FEMS Microbiol. Lett. 121*, 1−9.
5. Hendriks, J., Warne, A., Gohlke, U., Haltia, T., Ludovici, C., Lübben, M., and Saraste, M. (1998) The active site of the bacterial nitric oxide reductase is a dinuclear iron center, *Biochemistry 37*, 13102−13109.
6. Girsch, P., and deVries, S. (1997) Purification and initial kinetic and spectroscopic characterization of NO reductase from Paracoccus denitrificans, *Biochim. Biophys. Acta 1318*, 202−216.
7. Butland, G., Spiro, S., Watmough, N. J., and Richardson, D. J. (2001) Two conserved glutamates in the bacterial nitric oxide reductase are essential for activity but not assembly of the enzyme, *J. Bacteriol. 183*, 189−199.
8. Forte, E., Urbani, A., Saraste, M., Sarti, P., Brunori, M., and Giuffrè, A. (2001) The cytochrome cbb3 from Pseudomonas stutzeri displays nitric oxide reductase activity, *Eur. J. Biochem. 268*, 6486-6491.
9. Giuffrè, A., Stubauer, G., Sarti, P., Brunori, M., Zumft, W. G., Buse, G., and Soulimane, T. (1999) The heme-copper oxidases of Thermus thermophilus catalyze the reduction of nitric oxide: evolutionary implications, *Proc. Natl. Acad. Sci. U.S.A. 96*, 14718−14723.
10. Grönberg, K. L., Roldan, M. D., Prior, L., Butland, G., Cheesman, M. R., Richardson, D. J., Spiro, S., Thomson, A. J., and Watmough, N. J. (1999) A low-redox potential heme in the dinuclear center of bacterial nitric oxide reductase: implications for the evolution of energy-conserving heme-copper oxidases, *Biochemistry 38*, 13780−13786.
11. Moënne-Loccoz, P., and de Vries, S. (1998) Structural characterization of the catalytic high-spin heme b of nitric oxide reductase: A resonance Raman study, *J. Am. Chem. Soc. 120*, 5147−5152.
12. Kumita, H., Matsuura, K., Hino, T., Takahashi, S., Hori, H., Fukumori, Y., Morishima, I., and Shiro, Y. (2004) NO Reduction by Nitric-oxide Reductase from Denitrifying Bacterium Pseudomonas aeruginosa: Characterization of reaction intermediates that appear in the single turnover cycle, *J. Biol. Chem. 279*, 55247−55254.
13. Hendriks, J. H., Jasaitis, A., Saraste, M., and Verkhovsky, M. I. (2002) Proton and electron pathways in the bacterial nitric oxide reductase, *Biochemistry 41*, 2331−2340.
14. Watmough, N. J., Cheesman, M. R., Butler, C. S., Little, R. H., Greenwood, C., and Thomson, A. J. (1998) The dinuclear center of cytochrome bo3 from Escherichia coli, *J. Bioenerg. Biomembr. 30*, 55−62.
15. Pinakoulaki, E., Gemeinhardt, S., Saraste, M., and Varotsis, C. (2002) Nitric-oxide reductase. Structure and properties of the catalytic site from resonance Raman scattering, *J. Biol. Chem. 277*, 23407−23413.
16. Pereira, M. M., Santana, M., and Teixeira, M. (2001) A novel scenario for the evolution of haem-copper oxygen reductases, *Biochim. Biophys. Acta 1505*, 185−208.
17. Ferguson-Miller, S., and Babcock, G. T. (1996) Heme-copper terminal oxidases, *Chem. Rev. 96*, 2889−2907.
18. Shapleigh, J. P., and Payne, W. J. (1985) Nitric oxide-dependent proton translocation in various denitrifiers, *J. Bacteriol. 163*, 837−840.
19. Kannt, A., Michel, H., Cheesman, M. R., Thomson, A. J., Dreusch, A. B., Körner, H., and Zumft, W. G. (1998) in *Biological electron-transfer chains: genetics, composition and mode of operation* (Canters, G. W., and Vijgenboom, E., Eds.) pp 297−291, Kluwer Academic Publishers, Dordrecht.
20. Fujiwara, T., and Fukumori, Y. (1996) Cytochrome cb-type nitric oxide reductase with cytochrome c oxidase activity from Paracoccus denitrificans Atcc 35512, *J. Bacteriol. 178*, 1866−1871.
21. Sakurai, N., and Sakurai, T. (1997) Isolation and characterization of nitric oxide reductase from Paracoccus halodenitrificans, *Biochemistry 36*, 13809−13815.

22. Heiss, B., Frunzke, K., and Zumft, W. G. (1989) Formation of the N-N bond from nitric oxide by a membrane-bound cytochrome bc complex of nitrate-respiring (denitrifying) Pseudomonas stutzeri, *J. Bacteriol. 171*, 3288−3297.
23. Gibson, Q. H., and Greenwood, C. (1963) Reactions of cytochrome oxidase with oxygen and carbon monoxide, *Biochem. J. 86*, 541−554.
24. Proshlyakov, D. A., Pressler, M. A., and Babcock, G. T. (1998) Dioxygen activation and bond cleavage by mixed-valence cytochrome c oxidase, *Proc. Natl. Acad. Sci. U.S.A. 95*, 8020−8025.
25. Brzezinski, P., and Ädelroth, P. (1998) Pathways of proton transfer in cytochrome c oxidase, *J. Bioenerg. Biomembr. 30*, 99−107.
26. Verkhovsky, M. I., Morgan, J. E., Verkhovskaya, M. L., and Wikström, M. (1997) Translocation of electrical charge during a single turnover of cytochrome-c oxidase, *Biochim. Biophys. Acta 1318*, 6−10.
27. Tartof, K. D., and Hobbs, C. A. (1987) Improved media for growing plasmid and cosmid clones, *Bethesda Res. Lab. Focus 9*, 12.
28. Rosen, P., and Pecht, I. (1976) Conformational equilibria accompanying the electron transfer between cytochrome c (P551) and azurin from Pseudomonas aeruginosa, *Biochemistry 15*, 775−786.
29. Brändén, M., Sigurdson, H., Namslauer, A., Gennis, R. B., Ädelroth, P., and Brzezinski, P. (2001) On the role of the K-proton transfer pathway in cytochrome c oxidase, *Proc. Natl. Acad. Sci. U.S.A. 98*, 5013−5018.
30. Hendriks, J. H., Prior, L., Baker, A. R., Thomson, A. J., Saraste, M., and Watmough, N. J. (2001) Reaction of carbon monoxide with the reduced active site of bacterial nitric oxide reductase, *Biochemistry 40*, 13361−13369.
31. Oliveberg, M., Brzezinski, P., and Malmström, B. G. (1989) The effect of pH and temperature on the reaction of fully reduced and mixed-valence cytochrome c oxidase with dioxygen, *Biochim. Biophys. Acta 977*, 322−328.
32. Verkhovsky, M. I., Morgan, J. E., and Wikström, M. (1994) Oxygen binding and activation: early steps in the reaction of oxygen with cytochrome c oxidase, *Biochemistry 33*, 3079−3086.
33. Pinakoulaki, E., and Varotsis, C. (2003) Time-resolved resonance Raman and time-resolved step-scan FTIR studies of nitric oxide reductase from Paracoccus denitrificans: comparison of the heme b3-FeB site to that of the heme-CuB in oxidases, *Biochemistry 42*, 14856−14861.
34. Verkhovsky, M. I., Morgan, J. E., Puustinen, A., and Wikström, M. (1996) Kinetic trapping of oxygen in cell respiration, *Nature 380*, 268−270.
35. Field, S. J., Prior, L., Roldan, M. D., Cheesman, M. R., Thomson, A. J., Spiro, S., Butt, J. N., Watmough, N. J., and Richardson, D. J. (2002) Spectral properties of bacterial nitric-oxide reductase: resolution of pH-dependent forms of the active site heme b3, *J. Biol. Chem. 277*, 20146−20150.
36. Moënne-Loccoz, P., Richter, O. M. H., Huang, H. W., Wasser, I. M., Ghiladi, R. A., Karlin, K. D., and de Vries, S. (2000) Nitric oxide reductase from Paracoccus denitrificans contains an oxo-bridged heme/non-heme diiron center, *J. Am. Chem. Soc. 122*, 9344−9345.
37. Ädelroth, P., Ek, M., and Brzezinski, P. (1998) Factors determining electron-transfer rates in cytochrome c oxidase: investigation of the oxygen reaction in the R. sphaeroides enzyme, *Biochim. Biophys. Acta 1367*, 107−117.
38. Brändén, G., Brändén, M., Schmidt, B., Mills, D. A., Ferguson-Miller, S., and Brzezinski, P. (2005) The protonation state of a heme propionate controls electron transfer in cytochrome c oxidase, *Biochemistry*, in press.
39. Dermastia, M., Turk, T., and Hollocher, T. C. (1991) Nitric oxide reductase. Purification from Paracoccus denitrificans with use of a single column and some characteristics, *J. Biol. Chem. 266*, 10899−10905.

BI050524H